(12)

DNA-TR-81-290

$E_{||}$ EFFECTS ON PLASMA SHEAR ACROSS MAGNETIC FLUX TUBES

Ralph W. Kilb
Mission Research Corporation
P.O. Drawer 719
Santa Barbara, California 93102

26 October 1983

Technical Report

CONTRACT No. DNA 001-81-C-0060

THIS WORK WAS SPONSORED BY THE DEFENSE NUCLEAR AGENCY
UNDER RDT&E RMSS CODE B322082466 S99QAXHC00055 H2590D.

Prepared for
Director
DEFENSE NUCLEAR AGENCY
Washington, DC 20305

Destroy this report when it is no longer needed. Do not return to sender.

PLEASE NOTIFY THE DEFENSE NUCLEAR AGENCY, ATTN: STTI, WASHINGTON, D.C. 20305, IF YOUR ADDRESS IS INCORRECT, IF YOU WISH TO BE DELETED FROM THE DISTRIBUTION LIST, OR IF THE ADDRESSEE IS NO LONGER EMPLOYED BY YOUR ORGANIZATION.

UNCLASSIFIED

SECURITY CLASSIFICATION OF THIS PAGE (When Data Entered)

REPORT DOCUMENTATION PAGE	READ INSTRUCTIONS BEFORE COMPLETING FORM
1. REPORT NUMBER: DNA-TR-81-290	2. GOVT ACCESSION NO.: AD A141 339
3. RECIPIENT'S CATALOG NUMBER:	
4. TITLE (and Subtitle): $E_{\parallel}$ EFFECTS ON PLASMA SHEAR ACROSS MAGNETIC FLUX TUBES	5. TYPE OF REPORT & PERIOD COVERED: Technical Report
	6. PERFORMING ORG. REPORT NUMBER: MRC-R-770
7. AUTHOR(s): Ralph W. Kilb	8. CONTRACT OR GRANT NUMBER(s): DNA 001-81-C-0060
9. PERFORMING ORGANIZATION NAME AND ADDRESS: Mission Research Corporation, PO Drawer 719, Santa Barbara, California 93102	10. PROGRAM ELEMENT, PROJECT, TASK AREA & WORK UNIT NUMBERS: Task S99AXHC-00055
11. CONTROLLING OFFICE NAME AND ADDRESS: Director, Defense Nuclear Agency, Washington DC 20305	12. REPORT DATE: 26 October 1983
	13. NUMBER OF PAGES: 42
14. MONITORING AGENCY NAME & ADDRESS (if different from Controlling Office)	15. SECURITY CLASS (of this report): UNCLASSIFIED
	15a. DECLASSIFICATION/DOWNGRADING SCHEDULE: N/A since UNCLASSIFIED

16. DISTRIBUTION STATEMENT (of this Report)

Approved for public release, distribution unlimited.

17. DISTRIBUTION STATEMENT (of the abstract entered in Block 20, if different from Report)

18. SUPPLEMENTARY NOTES

This work was sponsored by the Defense Nuclear Agency under RDT&E RMSS Code B322082466 S99QAXHC00055 H2590D.

19. KEY WORDS (Continue on reverse side if necessary and identify by block number)

Nuclear Bursts
Striations
Ionosphere
Magnetosphere
Beta-tube Motion
E-fields Parallel-to-B ($E_{\parallel}$)
Variance of Electron Density

20. ABSTRACT (Continue on reverse side if necessary and identify by block number)

Necessary conditions are derived if very long plasma filaments (striations) are to remain magnetic flux tube aligned in distorted geomagnetic fields subsequent to nuclear burst. Special $E_{\parallel}$ fields are required, unrelated to resistive effects. It is not yet clear if such special $E_{\parallel}$ fields can appear in reality. If such special $E_{\parallel}$

DD FORM 1 JAN 73 1473 EDITION OF 1 NOV 65 IS OBSOLETE

UNCLASSIFIED

SECURITY CLASSIFICATION OF THIS PAGE (When Data Entered)

20. ABSTRACT (Continued)

fields cannot exist, long nuclear burst striations in the magnetosphere will gradually shear across magnetic flux tubes, break up into several shorter segments, descend into the lower ionosphere, and be consumed faster there by molecular deionization.

SUMMARY

An important question concerning the late-time evolution of nuclear burst plasma plumes and striations is how accurately the plasma filaments stay aligned with magnetic flux tubes as the filaments move about. Because of various forces acting on the plasma, time-varying currents are induced in the plasma that more or less distort the magnetic flux tubes. The existence of plasma currents also means that the ions and electrons do not move with exactly the same velocity. The question we wish to address here is the following: given a very long plasma filament aligned perfectly with a particular magnetic flux tube at some initial time, how accurately will the plasma elements of the filament be aligned along a single flux tube at later times?

There is a strong tendency for an ideal MHD plasma to move about in such a manner as to stay aligned with a magnetic flux tube. For example, a low energy density plasma moves transverse to $\vec{B}$ with a velocity nearly equal to $c\vec{E}\times\vec{B}/B^2$, and it has been shown[1,2] that one can consider the magnetic flux tubes to move with this same velocity if $\nabla\times\vec{E}_{\parallel}$ happens to be zero or parallel-to-$\vec{B}$ at all times. Within these approximations, one can then consider the plasma filaments and magnetic flux tubes to remain aligned at all times.

However, the existence of plasma currents implies that the ions and electrons do not both accurately follow the $c\vec{E}\times\vec{B}/B^2$ drift velocity, and that resistive or anomalous $\vec{E}_{\parallel}$ fields may occur whose $\nabla\times\vec{E}_{\parallel}$ may not be parallel-to-$\vec{B}$. Consequently, a long plasma filament originally aligned with a magnetic flux tube will not necessarily map onto a single flux tube at later times. It is this time-evolving shear of a plasma filament onto

several flux tubes that we investigate here because it could substantially speed up the late-time decay of nuclear burst striations by allowing a long filament to break up into several segments that can more easily fall into the lower ionosphere and be consumed by molecular chemistry there.

We show that special $\vec{E}_\parallel$ fields would be required if striations are to remain magnetic flux tube aligned. We have not yet been able to demonstrate that such special $\vec{E}_\parallel$ fields can appear in reality. Some observed auroral $\vec{E}_\parallel$ fields seem similar to our special $\vec{E}_\parallel$ fields. The observed westward motion of the Checkmate and Kingfish beta tubes may be consistent with a temporary appearance of these special $\vec{E}_\parallel$ fields, but further detailed computations are required to reach a definite conclusion.

If the above special $\vec{E}_\parallel$ fields cannot develop in nuclear burst striations, then it seems likely that long striations will gradually shear across adjacent flux tubes in those regions of the striation where $\vec{J}_\perp$ is non-zero, with a transverse-to-B shearing velocity equal to $c\vec{J}_\perp/eN$. The effect on the striated nuclear burst plasma would be to decrease the mean electron density $\overline{N}$ and rms electron density fluctuations σ_N at very high altitudes, to increase the $\overline{N}$ and σ_N at ionospheric altitudes, and to accelerate the overall plasma decay due to the more rapid molecular chemistry at ionospheric heights.

We show that in ionospheric plasmas the electrons move in direction of $\vec{J}_\perp$ relative to the background neutrals. This is contrary to the folklore of plasma theorists that "the ions carry the transverse-to-B currents". Thus, predictions of image striations in the E-layer may be a spurious result of theorists if the above special $E_\parallel$ fields could appear in actual plasmas.

PREFACE

The author benefited from many lengthy and stimulating discussions of this material with F. Fajen, R. Stagat, W. White, C. Longmire and J. Sperling. Briefer, but useful, discussions were also held with D. Maloof, T. Mazurek, D. Sowle, L. Wittwer and N. Krall. The author is also indebted to W. Chesnut, J. Workman and C. Prettie for information concerning Checkmate beta-tubes and Barium cloud striation behavior.

Due to the vociferous discussions unleashed by a preliminary version of this report (dated 30 June 1983), the present version has been revised to clarify the need for special E_1 fields if "image striations" are to be suppressed.

TABLE OF CONTENTS

LIST OF ILLUSTRATIONS

SECTION 1
DRIFT VELOCITY OF ELECTRONS, IONS, AND FLUX TUBES

We assume the electron fluid and ion fluid can be described by the usual fluid MHD equations (at least in the transverse-to-$\vec{B}$ directions) and Maxwell's equations. The two momentum equations for the electron fluid and ion fluid can be inverted to express the transverse-to-$\vec{B}$ electron velocity $\vec{V}_{e\perp}$ and ion velocity $\vec{V}_{i\perp}$ in terms of $\vec{E}_\perp$, the neutral wind velocity $\vec{V}_{o\perp}$, the Pedersen conductivity σ_p and Hall conductivity σ_h, ion fluid acceleration, gravity, pressure gradients, etc. The exact expressions are algebraically very complex, and are given on pages 617-621 of Reference 3. For convenience of the reader, this section of Reference 3 is reproduced as an addendum to this note. For particular model problems, one usually will simplify the full equations (12-133, 12-134, and 12-135) for the relevant physical problem being investigated.

Newcomb[1] has shown how one may ascribe a velocity field $\vec{V}_{f\perp}$ for the motion of magnetic flux tubes when $\vec{E}_\perp$ and $\vec{E}_\parallel$ fields are present. Because the flux tubes are not true entities, there is some degree of arbitrariness to this velocity field which one can exploit in particular problems, e.g., by matching $\vec{V}_{f\perp}$ to $\vec{V}_{e\perp}$ or $\vec{V}_{i\perp}$ on some convenient surface that cuts through all the magnetic field lines (see Figure 1).

Given $\vec{E}_\perp$ and $\vec{E}_\parallel$ over the magnetic volume of interest, Newcomb showed that the flux tube velocity is:

$$\vec{V}_{f\perp} = -\frac{c}{B^2}\,\vec{B}\times\left[\,\vec{E}_\perp - \nabla_\perp \int_0^{\ell_\parallel} E_\parallel d\ell_\parallel + \nabla_\perp f(x_s, y_s, \ell_\parallel = 0)\,\right] \qquad (1)$$

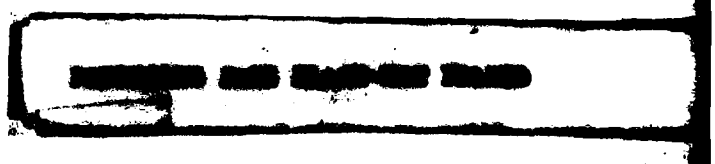

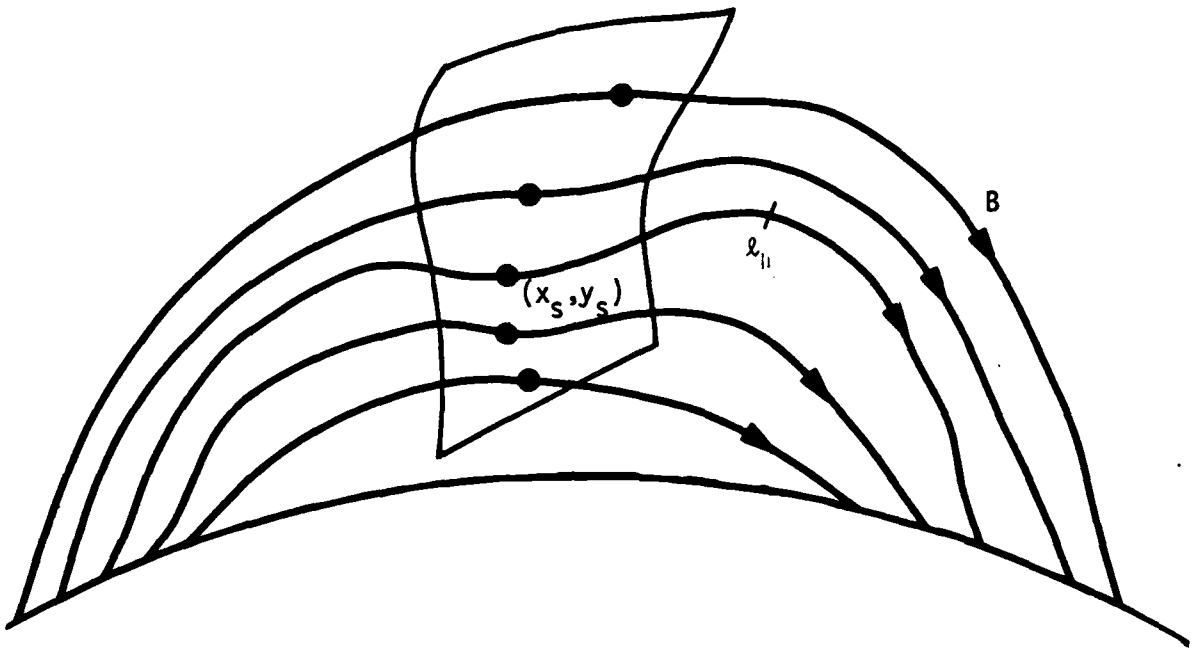

Figure 1. Distorted geomagnetic field lines and an example of a chosen surface that cuts all relevant field lines. A particular field line is identified by the coordinates x_s and y_s in the surface where the field line cuts through the surface, and $\ell_{\parallel}$ is the distance along the field line from that surface point.

Here x_s and y_s are surface coordinates in a chosen surface that cuts through all the magnetic field lines, and the line integral $\int E_\parallel d\ell_\parallel$ is to be evaluated along each magnetic field line, starting at the point where the field line cuts through the surface (i.e., $\ell_\parallel \equiv 0$ there). The arbitrariness of the $\vec{V}_{f\perp}$ is given by the term $\nabla_\perp f(x_s, y_s, \ell_\parallel = 0)$, where $f(x_s, y_s)$ may be any desired function defined on the chosen surface. Usually it is desirable to place the surface where $\vec{E}_\parallel$ is negligible and choose f=0; near this surface Equation 1 then yields $\vec{V}_{f\perp} = c\vec{E}_\perp \times \vec{B}/B^2$, but more distant points from this surface will also have a contribution from the second term of Equation 1.

Equation 1 satisfies Faraday's law because:

$$\frac{\partial \vec{B}}{\partial t} = -c\nabla \times \vec{E}$$

$$= -c\nabla \times [\vec{E} + \nabla f(x_s, y_s, \ell_\parallel)]$$

$$= \nabla \times (\vec{V}_f \times \vec{B}) \qquad (2)$$

Newcomb points out that the last step is valid if we choose

$$\nabla_\parallel f(x_s, y_s, \ell_\parallel) = -\vec{E}_\parallel(x_s, y_s, \ell_\parallel) \qquad (3)$$

which on integration along the field lines starting from our surface (at $\ell_\parallel = 0$) yields

$$f(x_s, y_s, \ell_\parallel) = f(x_s, y_s, \ell_\parallel = 0) - \int_0^{\ell_\parallel} E_\parallel d\ell_\parallel \qquad (4)$$

where $f(x_s, y_s, \ell_\parallel = 0)$ may be chosen arbitrarily on the surface that cuts all field lines. Consequently from Equations 2 and 3:

$$\vec{V}_{f\perp} \equiv -\frac{c}{B^2}\vec{B}\times[\vec{E} + \nabla f(x_s, y_s, \ell_\parallel)]$$

$$= -\frac{c}{B^2}\vec{B}\times[\vec{E}_\perp - \nabla_\perp \int_0^{\ell_\parallel} E_\parallel d\ell_\parallel + \nabla_\perp f(x_s, y_s, \ell_\parallel = 0)] \quad (5)$$

Thus this velocity field describes exactly the evolution of the magnetic field if we are given $\vec{E}_\perp$ and $\vec{E}_\parallel$ at all times and at all locations.

How much a plasma filament becomes misaligned from a flux tube depends on how much the ion velocity $\vec{V}_{i\perp}$ or electron velocity $\vec{V}_{e\perp}$ deviates from the flux tube velocity $\vec{V}_{f\perp}$ at different points along the flux tube, given that the plasma velocity and flux tube velocity are set equal at a chosen surface that cuts across all field lines. Comparing Equations 12-133 and 12-134 of the addendum with Equation 5 above, it seems likely that some deviations exist between these three transverse-to-B velocity vectors. However, these general equations are so complex that it is difficult to come to specific conclusions. Thus we will examine a couple of simple problems to exemplify possible plasma motion.

SECTION 2
EXAMPLE OF IONOSPHERIC PLASMA MOTION

Let us consider a plasma in the lower ionosphere where the dominant forces are collisions of ions and electrons with neutrals. Thus in Equations 12-125 and 12-126 of the addendum we neglect the inertial terms, the pressure gradients, and gravitational force, so momentum balance for the ion and electron fluids is:

$$0 = eN(\vec{E}+\vec{V}_i\times\vec{B}/c) + \nu_{io}\rho_i(\vec{V}_o-\vec{V}_i) - \nu_{ei}\rho_e(\vec{V}_i-\vec{V}_e) \tag{6}$$

$$0 = -eN(\vec{E}+\vec{V}_e\times\vec{B}/c) + \nu_{eo}\rho_e(\vec{V}_o-\vec{V}_e) + \nu_{ei}\rho_e(\vec{V}_i-\vec{V}_e) \tag{7}$$

Addition of these two equations yields

$$0 = \vec{J}\times\vec{B} + \nu_{io}\rho_i(\vec{V}_o-\vec{V}_i) + \nu_{eo}\rho_e(\vec{V}_o-\vec{V}_e) \tag{8}$$

where we have employed the definition

$$\vec{J} = \frac{eN}{c}(\vec{V}_i-\vec{V}_e) \tag{9}$$

We can now express $\vec{V}_{i\perp}$, $\vec{V}_{e\perp}$ $\vec{E}_\perp$ and $\vec{V}_{f\perp}$ in terms of $\vec{J}_\perp$, the neutral wind velocity $\vec{V}_{o\perp}$, and the magnitudes of the ratios of collision frequencies over gyro frequencies ($n_{io}=\nu_{io}/\Omega_i$, $n_{eo}=\nu_{eo}/\Omega_e$, and $n_{ei}=\nu_{ei}/\Omega_e$) by the following procedure: (a) use Equation 9 to eliminate V_e in Equation 8 and solve for $\vec{V}_{i\perp}$; (b) use the resultant equation and Equation 9 to express

$\vec{V}_{e\perp}$ in terms of $\vec{J}_\perp$ and $\vec{V}_{o\perp}$; (c) then use Equations 6 or 7 to find $\vec{E}_\perp$, and Equation 5 to find $\vec{V}_{f\perp}$. The resultant expressions are:

$$\vec{V}_{i\perp} = \vec{V}_{o\perp} + \frac{1}{n_{io}+n_{eo}} \cdot \frac{c\vec{J}\times\vec{b}}{eN} + \frac{n_{eo}}{n_{io}+n_{eo}} \cdot \frac{c\vec{J}_\perp}{eN} \tag{10}$$

$$\vec{V}_{e\perp} = \vec{V}_{o\perp} + \frac{1}{n_{io}+n_{eo}} \cdot \frac{c\vec{J}\times\vec{b}}{eN} - \frac{n_{io}}{n_{io}+n_{eo}} \cdot \frac{c\vec{J}_\perp}{eN} \tag{11}$$

$$\vec{V}_{f\perp} = \vec{V}_{o\perp} + \left[\frac{1+n_{io}n_{eo}}{n_{io}+n_{eo}} + n_{ei} \right] \frac{c\vec{J}\times\vec{b}}{eN} - \frac{c}{B} \vec{b}\times\nabla_\perp f(x_s, y_s, 0)$$

$$- \frac{n_{io}-n_{eo}}{n_{io}+n_{eo}} \cdot \frac{c\vec{J}_\perp}{eN} + \frac{c}{B} \vec{b}\times\nabla_\perp \int E_\parallel \, d\ell_\parallel \tag{12}$$

$$\vec{E}_\perp = - \frac{\vec{V}_o\times\vec{B}}{c} + \left[\frac{1+n_{io}n_{eo}}{n_{io}+n_{eo}} + n_{ei} \right] \frac{B\vec{J}_\perp}{eN} + \frac{n_{io}-n_{eo}}{n_{io}+n_{eo}} \cdot \frac{\vec{J}\times\vec{B}}{eN} \tag{13}$$

No approximations have been made in deriving Equations 10-13 from Equations 5-9, except that the electron density N_e is very nearly equal to the ion density N_i.

Note that the first two terms in Equations 10 and 11 for $\vec{V}_{i\perp}$ and $\vec{V}_{e\perp}$ are the same. The last term of Equations 10 and 11 shows the velocity components of $\vec{V}_{i\perp}$ and $\vec{V}_{e\perp}$ in direction of $\vec{J}_\perp$; because $n_{io} \approx 1000 n_{eo}$ at all altitudes, this shows that the <u>electrons</u> carry essentially all of the transverse-to-B current density relative to the neutrals.

More precisely, the vector dot products of $\vec{J}_\perp$ with Equations 10 and 11 show that <u>in a reference frame moving with the local neutral wind velocity</u> $\vec{V}_{0\perp}$, it is essentially only the electrons that move in direction of $\vec{J}_\perp$ and the ions have essentially no motion in the $\vec{J}_\perp$ direction. The writer dearly hopes that consideration of Equations 10 and 11 will lay to rest the hoary tale of plasma theorists that "the ions carry the $\vec{J}_\perp$ because the ion Pedersen conductivity is a 1000-fold larger than the electron Pedersen conductivity". Ionospheric theorist seem more at home with equations expressed in terms of $\vec{E}_\perp$ and $\vec{E}\times\vec{b}$; such an alternative derivation is given in the Appendix, again showing that $\vec{J}_\perp \cdot \vec{V}_{i\perp}$ is very small compared to $\vec{J}_\perp \cdot \vec{V}_{e\perp}$ in the reference frame of the neutral fluid.

Because the $\vec{J}_\parallel$ is also carried primarily by the electrons, Equations 10 and 11 show that the current density $\vec{J}$ is a result of primarily electron motion around the whole current circuit.

Let us consider now the conditions needed such that a plasma filament will stay field-aligned during its drift motion. This means that we would like the flux tube velocity $\vec{V}_{\perp f}$ to be equal to either the ion velocity $\vec{V}_{i\perp}$ or the electron velocity $\vec{V}_{e\perp}$. Comparing the second term of Equation 12 with that of Equations 10 and 11, we see that we must have $\eta_{eo}=0$ and $\eta_{ei}=0$, i.e., electron collision should be negligible. (This is in line with the usual expectation of theorists.) In this limit, the next-to-last term of Equation 12 reduces to $-c\vec{J}_\perp/eN$, so the magnetic flux tubes could move with the electrons if the last term of Equation 12 were negligible, e.g., if $E_\parallel$ were zero. The flux tubes would distort if they follow the electron $\vec{V}_{e\perp}$ that is consistent with the plasma motion and the $\vec{J}_\perp$. In this case ($E_\parallel=0$ and $\eta_{eo}=\eta_{ei}=0$) "image striations" can form in regions where $\nabla\cdot\vec{V}_{e\perp}$ is non-zero.

Alternatively, the magnetic flux tubes might follow the ion motion (i.e., $\vec{V}_{f\perp}=\vec{V}_{i\perp}$). In addition to requiring no electron collisions, the continuing alignment of the ion fluid and a flux tube requires that the last two terms of Equations 12 cancel each other. Crossing these last two terms with $\vec{B}$, this requires:

$$\nabla_\perp \int_0^{\ell_\parallel} E_\parallel d\ell_\parallel = \frac{n_{io}-n_{eo}}{n_{io}+n_{eo}} \cdot \frac{\vec{J}\times\vec{B}}{eN} \qquad (14)$$

Thus the presence of current loops in this case requires the appearance of special $\vec{E}_\parallel$ fields if the ion fluid is to stay flux-tube aligned. These special $\vec{E}_\parallel$ fields do not seem to be associated with any resistive effects associated with $\vec{J}_\parallel$. In fact, Equation 14 must hold in the limit of no electron collisions if the ion fluid is to stay flux tube aligned. In this case no "image striations" can form because the electrons move across the magnetic flux tubes in direction of $\vec{J}_\perp$.

It is noteworthy that the r.h.s. of Equation 14 is exactly the same term as the last term of Equation 13 for $\vec{E}_\perp$. This last term for $\vec{E}_\perp$ appears to be that part of $\vec{E}_\perp$ required so that the electrons can "$\vec{E}\times\vec{B}$" drift across the plasma and thus generate the current density $\vec{J}_\perp$, i.e., the last term of Equation 11. Denoting this last term of Equation 13 (which is along the direction $\vec{J}\times\vec{B}$) as $\vec{E}_{\perp J\times B}$, we can then rewrite Equation 14 as:

$$\nabla_\perp \int_0^{\ell_\parallel} E_\parallel d\ell_\parallel = \vec{E}_{\perp J\times B} \qquad (15)$$

Taking the derivative of this equation w.r.t. $\ell_\parallel$, this appears to imply:

$$\nabla\times(\vec{E}_{\parallel} + \vec{E}_{\perp J\times B}) = 0 \qquad (16)$$

Thus we see that the purpose of the special $\vec{E}_{\parallel}$, required by Equation 14, is to cancel any non-zero curl of the last term of $\vec{E}_{\perp}$ in Equation 13 and thereby suppress the associated $\partial\vec{B}/\partial t$. That is, that portion of the total $\vec{E}$ field that appears in Equation 16 must be the gradient of a potential:

$$\vec{E}_{\parallel} + \vec{E}_{\perp J\times B} = -\nabla\phi \qquad (17)$$

Although the above discussion may strike the reader as somewhat bizarre, there appears to be a theoretical similarity with $E_{\parallel}$ fields that are observed to be associated with auroral arcs. For example, see the discussion of auroral $E_{\parallel}$ fields by Hallinan[4].

The time evolution of the plasma motion and magnetic field configuration can be computed from Equations 10 and 12 for $\vec{V}_{i\perp}$ and $\vec{V}_{f\perp}$, plus Ampere's Law ($\vec{J}=\nabla\times\vec{B}/4\pi$) and an expression for $E_{\parallel}$ (e.g., Equation 14 or electron momentum balance parallel-to-B). The distorting magnetic field lines are advanced in time by the integral of $\vec{V}_{f\perp}$, and $\vec{B}$ is computed from the spatially distorted field lines. Note that Equations 11 and 13 are not necessary to solve for the plasma and magnetic field evolution, but are merely auxiliary equations that allow the computation of $\vec{V}_{e\perp}$ and $\vec{E}_{\perp}$ if these quantities are desired. This procedure conforms with Faraday's law ($\partial\vec{B}/\partial t=-c\nabla\times\vec{E}$) because of the above choice for $\vec{V}_{f\perp}$.

SECTION 3
A SIMPLIFIED DETAILED EXAMPLE

The rising Kingfish fireball and associated kinked beta-tube ought to be described fairly well by Equations 10-13. Thus if we were given the density ρ_0 and velocity $\vec{V}_0$ of the neutrals, and the ion number density N in the fireball and the beta-tube, then the above equations should predict the evolution of the plasma location and magnetic field configuration. The beta tube behavior was clearly visible below ≈120 km altitude, and clearly showed that field lines leaving the high altitude fireball were highly distorted down to about 85 km altitude for about three minutes after the burst. A peculiarity of the data is that the footpoints of these field lines, at ≈85 km altitude, moved about 50 km westward of the fireball magnetic meridian, as well as lagging behind the fireball rise in their northward motion. The upward bend of these field lines at ≈85 km altitude was as much as 45°, so a substantial current loop was set up linking the high altitude fireball plasma to the beta-tube kink down at 85 km altitude.

An explicit computation of the Kingfish behavior is beyond the scope of the present paper, but we shall consider a model problem that I believe retains the essence of the Kingfish problem, and therefore will allow us to compare with the observed field line behavior. Figure 2 shows the model plasma and neutral wind configuration. The figure might correspond to a nuclear burst in the lower ionosphere at the geomagnetic equator, wherein the central plasma represents the fireball and the northern and southern plasmas represent the northern and southern conjugate region (NCR and SCR) beta-tube plasmas. Here we are in a reference frame moving upward with 1/2 of the fireball velocity.

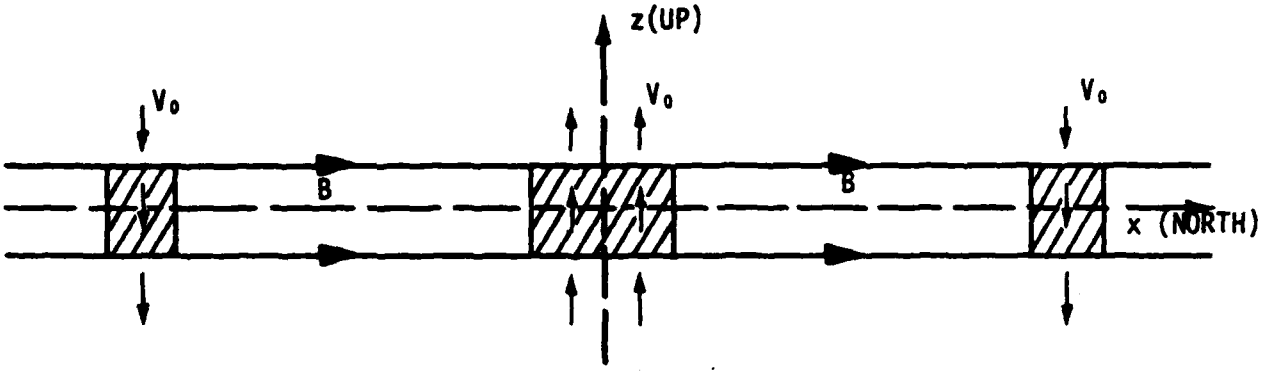

(a). Initial configuration. View from east.

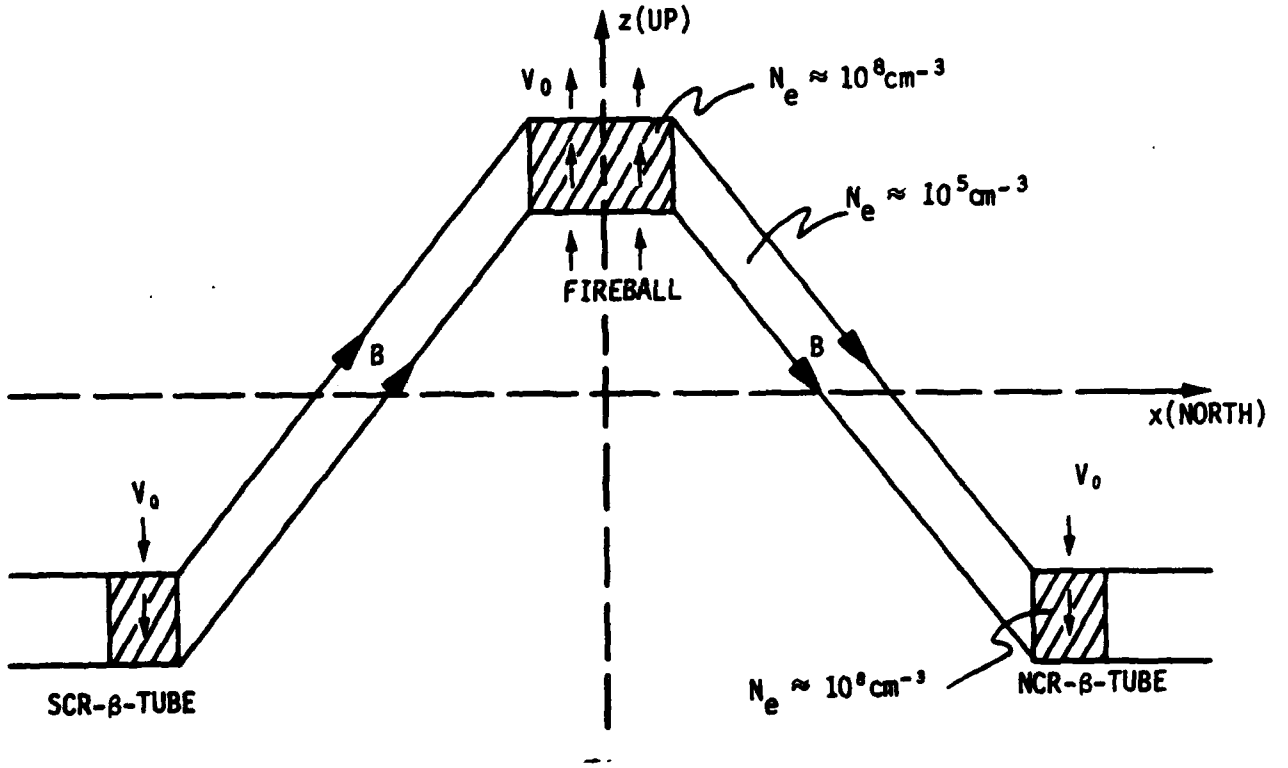

(b). Final quasi-steady state configuration. View from east.

Figure 2. Model plasma that exemplifies the Kingfish bent beta-tube problem.

In the model problem shown in Figure 2, there are three high density plasma elements along the initially undistorted magnetic flux tube, embedded in a background of low density plasma. As an example, the three high density regions might have 10^8 ions/cm^3, and the surrounding low density plasma might have 10^5 ions/cm^3. The z-axis is vertical (e.g., located at the geomagnetic equator), while the x-axis is horizontal and pointing northward. We assume the length of the central plasma element is twice the length of the two equally long northern and southern elements. The neutral fluid density is assumed uniform everywhere, and there is an upward neutral fluid velocity V_0 across the central plasma element, and an equal but downward velocity $-V_0$ across the northern and southern plasma elements. Consequently there is an east-west vertical plane of symmetry across the middle of the central plasma (say at x=0), and we need consider only the details of the northern half of the model problem.

Figure 2a shows the configuration at the initial instant when the vertical neutral winds are turned on. If the three plasma elements stayed aligned within a common distorted magnetic flux tube, it would eventually take on the quasi-steady state configuration shown in Figure 2b.

Figure 3 shows the current configuration for the case when the transverse-to-B plasma cross-section is rectangular (say 10km×10km). The top view, shown in Figure 3a, shows a westward $J_\perp$ across the central plasma element; the associated downward $\vec{J}_\perp \times \vec{B}$ force balances the large upward ion-neutral drag force (the second term of Equation 8) and thereby determines $\vec{V}_{i\perp}$ at any instant. When this $J_\perp$ reaches the west face of the central plasma element, it turns into $J_\parallel$ that runs down the field lines to the northern (and southern) plasma element. There the $J_\parallel$ turns into an eastward $J_\perp$, whose associated upward $\vec{J}_\perp \times \vec{B}$ force balances the downward ion-neutral drag force there. When this $J_\perp$ reaches the east face of the

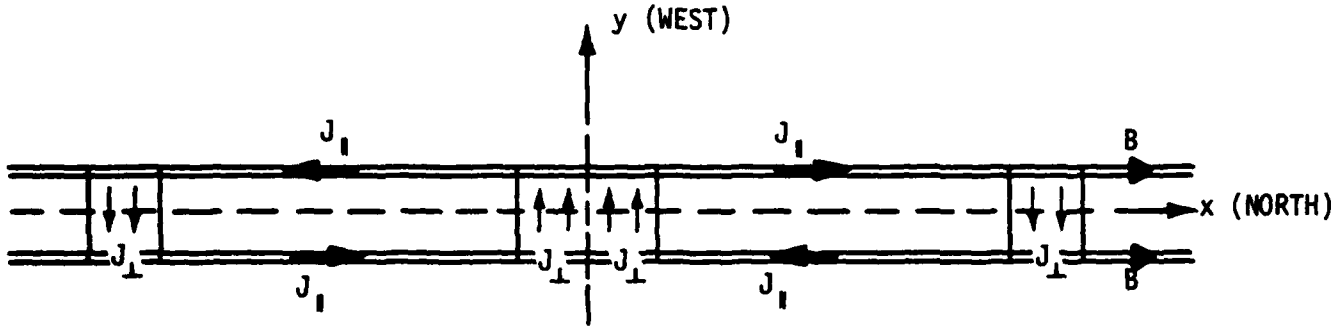

(a). Top view.

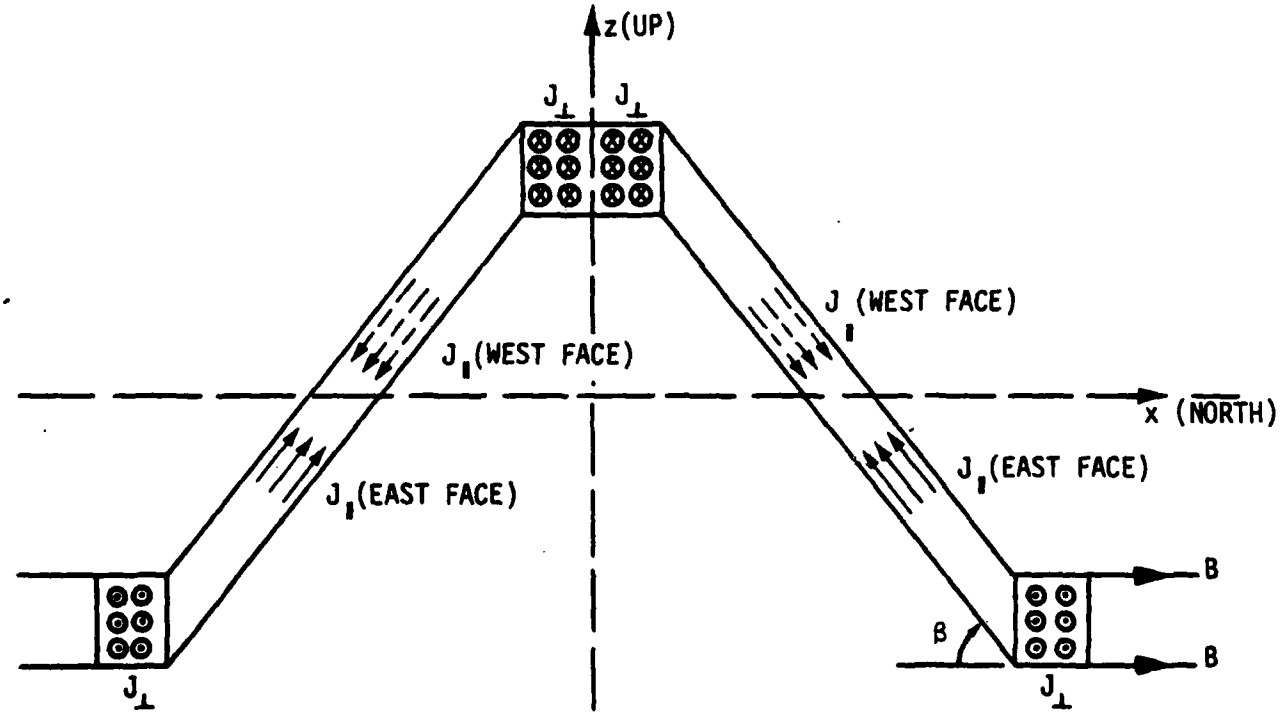

(b). View from east

Figure 3. Current paths in final quasi-steady state configuration.

northern plasma element, it turns into $J_\parallel$ and runs back up the field line to the central plasma element to complete the current circuit.

Figure 3b shows the distorted flux tube and $J_\perp$ directions as seen from the east. Note that the field lines are bent in the regions where $J_\perp$ flows. If the field lines are bent an angle β across the region of a plasma element, one can relate[4] the field-line-integrated $J_\perp$ to the kink angle β across the plasma element via Ampere's Law ($\vec{J}=\nabla\times\vec{B}/4\pi$):

$$\int J_\perp d\ell_\parallel = \frac{B}{4\pi} \sin\beta \tag{18}$$

We can use this expression to relate $\vec{V}_{i\perp}$ to the kink angle β across each plasma element by field-line-integrating Equation 8 along each plasma element. This yields for each plasma element

$$V_{i\perp} = \frac{\int n_{io} e N V_o d\ell_\parallel - cB\sin\beta/4\pi}{\int n_{io} e N d\ell_\parallel} \tag{19}$$

Assuming now that the flux tube distorts with the plasma velocity $V_{i\perp}$, the transverse-to-B displacement of each flux tube element is given by $\int V_{i\perp} dt$, and the resultant kinked flux tube geometry determines the various kink angles $\beta(t)$ as a function of time at each plasma element. Thus Equation 19 allows a complete computation of the flux tube evolution in time (assuming that it moves with the local ion fluid velocities $V_{i\perp}$). In particular, for our simple model problem, Equation 19 shows that a steady-state configuration ($V_{i\perp}=0$ everywhere) is reached when the flux tube becomes sufficiently kinked so that the numerator of Equation 19 is zero for each of the three plasma elements.

Assuming for the moment that there are no electron collisions (so that $n_{eo}=n_{ei}=0$), the electric field $\vec{E}_\perp$ in the quasi-steady state limit is given by the last term of Equation 13, because the first two terms

cancel in this limit. Figure 4 shows this $\vec{E}_{\perp J\times B}$ for the northern half of our model problem. Note that $\vec{E}_{\perp J\times B}$ is directed <u>downward</u> throughout the central plasma element, but <u>upward</u> throughout the entire northern element. This allows the electrons to "E×B" drift eastward in the central plasma element, and westward in the northern element, thus generating the corresponding $\vec{J}_\perp$ shown in Figure 3. The ions cannot follow this particular "E×B" drift because the ion-neutral collisional force $\nu_{io}\rho_i\vec{V}_{o\perp}$ in Equation 6 opposes this $\vec{E}_{\perp J\times B}$ field component.

Note that the $\vec{E}_{\perp J\times B}$ vector shown in Figure 4 actually points in opposite directions at different positions along the flux tube, i.e., at the central and the northern plasma elements. Thus this quasi-steady state configuration cannot be approximated by an equipotential solution. Furthermore, $\partial\vec{B}/\partial t$ must be negligible in our quasi-steady state, so Faraday's law requires $\nabla\times\vec{E}=0$. Because $\vec{E}_{\perp J\times B}$ is the only electric field component transverse-to-B, this implies that an $\vec{E}_\parallel$ must exist such that:

$$0 = \nabla\times(\vec{E}_\parallel+\vec{E}_{\perp J\times B}) = \nabla\times(\vec{E}_\parallel+\vec{J}\times\vec{B}/eN) \qquad (20)$$

because $\vec{E}_{\perp J\times B}$ is the last term of Equation 13 (in the limit that $n_{eo}=0$). This is consistent with the steady-state assumption that $\vec{V}_{f\perp}$ has no component in direction of $\vec{J}_\perp$, i.e., that the two terms on the second line of Equation 12 cancel one another (of course, the first two terms on the r.h.s. of Equation 12 also cancel one another in the quasi-steady state, but not during the initial transient stage when the flux tube and plasma elements have vertical motions).

The resultant quasi-steady state $\vec{E}_\parallel$ fields are indicated in Figure 4. Note that $\vec{E}_\parallel$ occurs primarily at the left and right edges of the plasma element where $\vec{E}_{\perp J\times B}$ undergoes strong changes. Furthermore, this $\vec{E}_\parallel$ exists across the whole east-west extent of the plasma element

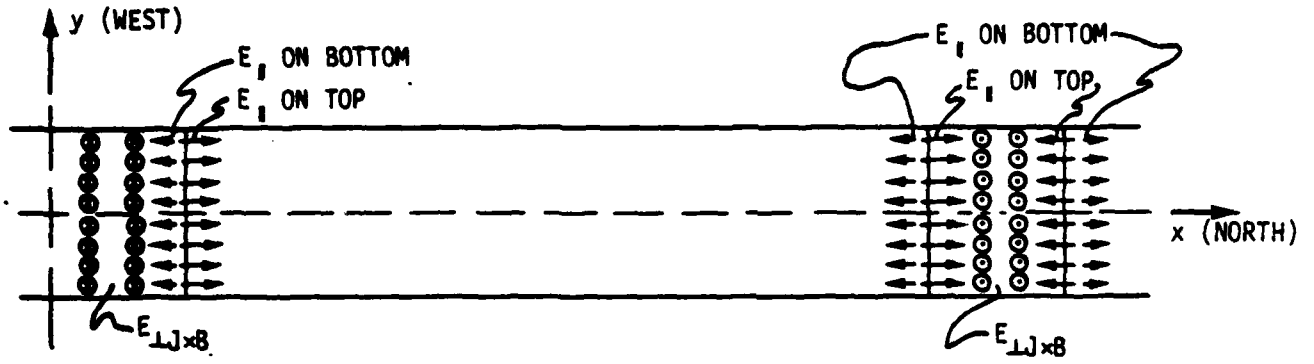

(a) Top view of northern half

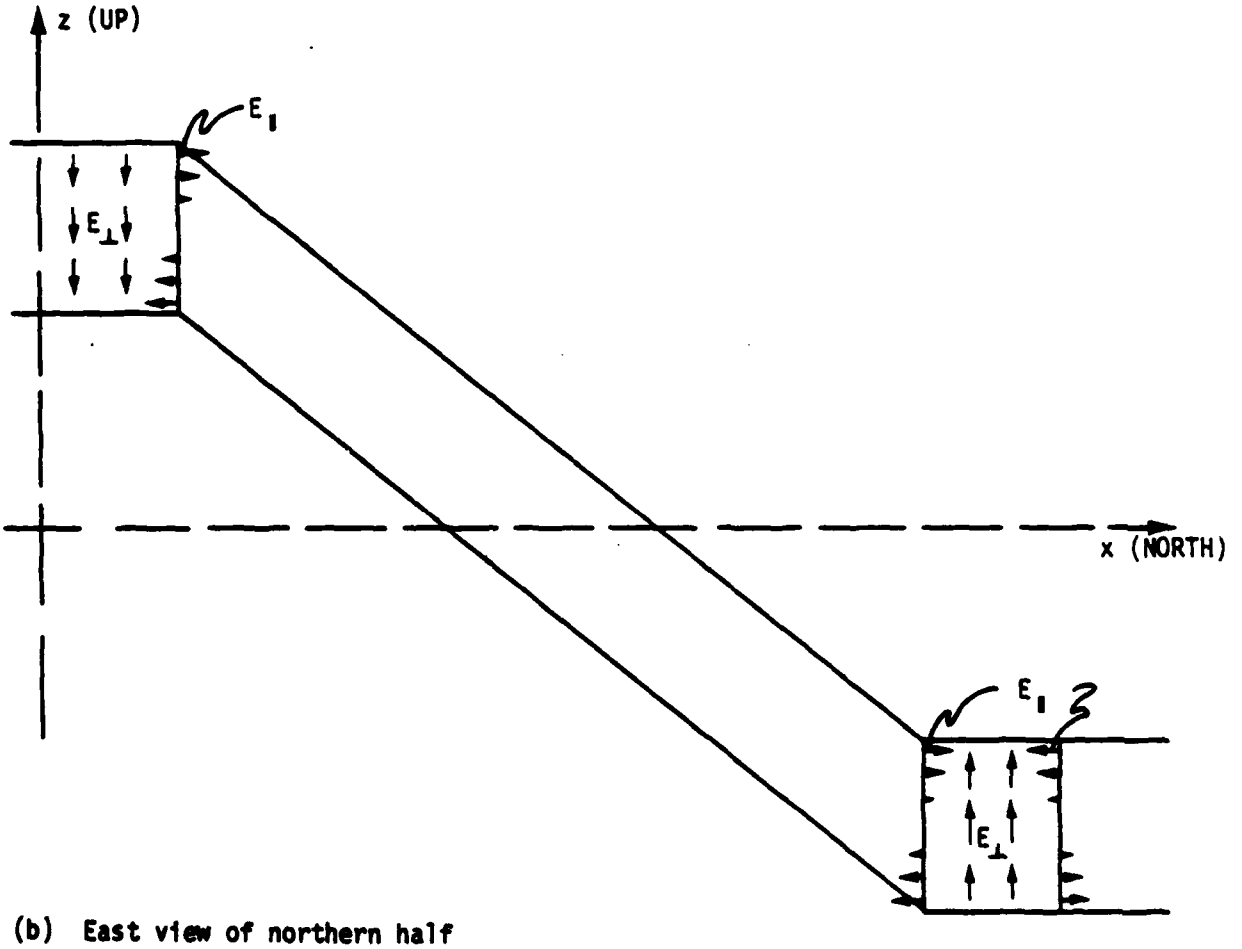

(b) East view of northern half

Figure 4. The $\vec{E}_{\perp J \times B}$ field and associated $\vec{E}_{\parallel}$ in final quasi-steady state configuration.

edges, and is in opposite directions at the top and bottom parts of the elements. The $\vec{E}_{\parallel}$ is also in opposite directions on the left and right sides of the plasma elements. Note that this $\vec{E}_{\parallel}$ is not at all correlated with the location of $\vec{J}_{\parallel}$, and in fact must exist, in this quasi-steady state configuration, even when electron collisions are negligible.

Let us now consider what would happen when electron collisions are allowed. To keep close to the Kingfish data, suppose electron collisions are still negligible in the central plasma element (i.e., the fireball plasma), but extensive electron collisions occur in the region of the northern plasma element (i.e., the NCR beta tube region). The second term of Equation 12 then indicates that the flux tube velocity $\vec{V}_{\perp f}$ would now have an additional term $(n_{eo}+n_{ei})c\vec{J}\times\vec{b}/eN$. For the northern plasma element, this additional velocity is upward, and therefore allows the distorted field line to relax toward the ambient (horizontal) configuration. This motion seems consistent with the northward migration of the Kingfish beta tube footpoint.

Electron collision effects in the next-to-last term of Equation 12 indicate a further additional term for $\vec{V}_{\perp f}$ equal to $2(n_{eo}/n_{io})c\vec{J}_{\perp}/eN$. Because $n_{io}\approx 1000 n_{eo}$, this latter term is quite negligible in magnitude compared to the previous additional term. Furthermore, this term is directed <u>eastward</u>, whereas the Kingfish (and Checkmate) beta tube footpoints clearly migrated about 50 km <u>westward</u> during its northward motion. Thus electron collisions involved in this term of Equation 12 cannot explain the observed westward beta tube migration.

The observed westward migration would be explained if the special $\vec{E}_{\parallel}$ discussed above were to diminish in part or wholly. In that case, $\vec{V}_{\perp f}$ would have an additional term equal to some fraction of $-c\vec{J}_{\perp}/eN$, and this is correctly directed in the westward direction in the northern

and southern plasma elements. The Kingfish data seems to imply, then, that the required special $\vec{E}_{\parallel}$ may have developed during the first 30 seconds after the burst when the beta-tube stayed locked in place, but at subsequent times it did not reach the required magnitude so as to cancel the $-c\vec{J}_{\perp}/eN$ term in Equation 12. The reason for this is not clear, but may be related to the substantially lower electron density N at the beta tube footprints at the later times.

SECTION 4
MAGNETOSPHERIC PLASMA

Let us now consider a plasma in the magnetosphere where collisions with neutrals are negligible. We will also neglect plasma pressure gradients and electron inertia, so ion and electron fluid momentum balance in the magnetosphere is approximated by the following two simplified versions of Equations 12-125 and 12-126 of the addendum:

$$\rho_i \dot{\vec{V}}_i = + eN(\vec{E}+\vec{V}_i \times \vec{B}/c) - \nu_{ei}\rho_e(\vec{V}_i - \vec{V}_e) \tag{21}$$

$$0 = - eN(\vec{E}+\vec{V}_e \times \vec{B}/c) + \nu_{ei}\rho_e(\vec{V}_i - \vec{V}_e) \tag{22}$$

Addition of these two equations yields

$$\rho_i \dot{\vec{V}}_i = \vec{J} \times \vec{B} \tag{23}$$

This equation may be solved for $\vec{J}_\perp$:

$$\vec{J}_\perp = \frac{\rho_i}{B} \vec{b} \times \dot{\vec{V}}_i \tag{24}$$

In the magnetospheric case, it is not possible to eliminate $\vec{E}_\perp$ in the equations for $\vec{V}_{i\perp}$ and $\vec{V}_{e\perp}$ via algebra (in analogy with Equations 10 and 11 for the ionospheric case). Here we must time-integrate Equation 23 to obtain $\vec{V}_{i\perp}(t)$, and use Equations 9 and 23 to relate $\vec{V}_{e\perp}(t)$ to $\vec{V}_{i\perp}(t)$:

$$\vec{V}_{i\perp}(t) = \vec{V}_{i\perp}(0) + \int_0^t dt\, \vec{J} \times \vec{B}/\rho_i \tag{25}$$

$$\vec{V}_{e\perp} = \vec{V}_{i\perp} + \dot{\vec{V}}_i \times \vec{b}/\Omega_i = \vec{V}_{i\perp} - c\vec{J}_\perp/eN \tag{26}$$

$$\vec{V}_{f\perp} = \vec{V}_{i\perp} + \eta_{ei} \frac{c\vec{J}\times\vec{b}}{eN} - \frac{c}{B}\vec{b}\times\nabla_\perp f(x_s, y_s, 0)$$

$$- \frac{c\vec{J}_\perp}{eN} + \frac{c}{B}\vec{b}\times\nabla_\perp \int E_\parallel \, d\ell_\parallel \tag{27}$$

$$\vec{E}_\perp = - \frac{\vec{V}_i \times \vec{B}}{c} + \eta_{ei} \frac{B\vec{J}_\perp}{eN} + \frac{\vec{J}\times\vec{B}}{eN} \tag{28}$$

The last two equations were obtained by solving Equations 21, 23 and 9 for $\vec{E}_\perp$, and using this expression in Equation 1 to obtain $\vec{V}_{f\perp}$. The above Equations 25-28 for a magnetospheric plasma are analogous with Equations 10-13 for an ionospheric plasma. The two sets of equations are quite similar, so much of the above discussion of flux tube motion adhering to ionospheric plasma motion and appearance of special $\vec{E}_\parallel$ fields also applies to the magnetospheric case.

For the magnetospheric case it is not immediately obvious that "the electrons carry the current" (when one is in an earth-fixed frame of reference). This does turn out to be approximately the case for simple shear Alfven waves. For example, Scholer considered the motion of a barium cloud in the magnetosphere[6], wherein he assumed that $\vec{J}_\perp$ was always pointed in one direction (although it could have plus or minus signs). Because Scholer assumed $\vec{V}_{i\perp}(0)=0$ and $\vec{J}\times\vec{B}$ was always in a single direction, Equation 25 shows that his $\vec{V}_{i\perp}$ did not ever have a component along $\vec{J}_\perp$. Consequently, one might infer that the electrons must carry the current in Scholer's problem (in his earth-fixed frame of reference). To

actually prove this, one has to retain the so-called "Hall inertial term" in the differential equations. The solution is then very difficult to obtain, but R. W. Stagat has been able to partly solve this complete differential equation for Scholer's problem.

Sperling[7] has derived an interesting analytical solution to an extension of Scholer's problem that also includes a special combination of ion and electron collisions with background neutrals. His solution explicitly shows the deviation of the flux tube motion from the plasma filament motion. In his paper, as in Scholer's, it was again assumed that $\vec{J}_\perp$ was always in one direction (with plus or minus signs), so one might again infer from Equation 25 that $\vec{V}_{i\perp}$ could not have a component along $J_\perp$.

If one grants that $\vec{V}_{i\perp}$ has essentially no component along $\vec{J}_\perp$ in the magnetospheric case, then Equation 27 shows that if the flux tube is to remain tied to the plasma filament, the last two terms of Equation 27 must cancel each other. Consequently, special $\vec{E}_\parallel$ fields would also be required in the magnetospheric plasma, just as in the ionospheric plasma. Also note that the last term of Equation 28 is the same $\vec{E}_{\perp J\times B}$ component of $\vec{E}_\perp$ as discussed in the ionospheric case. Thus all the above discussion for the ionospheric plasma can be applied analogously to the magnetospheric plasma.

The time evolution of the magnetospheric plasma and magnetic field line configuration can be computed via Equations 25 and 27 for $\vec{V}_{i\perp}$ and $\vec{V}_{f\perp}$, plus Ampere's law and an appropriate equation for $E_\parallel$. Here again, Equations 26 and 28 are merely auxiliary equations to compute $\vec{V}_{e\perp}$ and $\vec{E}_\perp$ if these quantities are desired.

SECTION 5
SUMMARY AND CONCLUSIONS

For ionospheric plasmas, it is clear that the electrons carry essentially all of the transverse-to-B currents as well as parallel-to-B currents relative to the neutral fluid. For magnetospheric plasmas the electrons also appear to be the primary current carrier, but this case is not so easily proven as that for ionospheric plasmas.

If the magnetic flux tubes were to remain aligned with the moving ion fluid, special $\vec{E}_{\parallel}$ fields must appear to cancel the curl of $\vec{E}_{\perp J\times B}$, where this component of $\vec{E}_{\perp}$ is defined to be the last term of Equation 13 or 28:

$$\vec{E}_{\perp J\times B} \equiv \vec{J}\times\vec{B}/eN \qquad (29)$$

This special $\vec{E}_{\parallel}$ is not associated with $\vec{J}_{\parallel}$, and it would have to exist even in the absence of electron collisions if the magnetic flux tube and plasma filament were to remain aligned. A consequence of these special $E_{\parallel}$ fields is that theorists' predictions of image striations in the lower ionosphere would be spurious. Such image striations have never been observed in the E-layer.

Unusual $\vec{E}_{\parallel}$ fields have been observed above the auroral zone, and these fields seem similar[4] to the $\vec{E}_{\parallel}$ discussed here.

The westward motion of the Kingfish and Checkmate beta-tubes, during the first three minutes after these nuclear bursts, may be consistent with the initial appearance of these special $\vec{E}_{\parallel}$ fields during the

first 30 seconds and their subsequent gradual decay. The specific computation of the decay of such $\vec{E}_{\parallel}$ fields is not understood, however, but it may involve the detailed evolution of the electron velocity distribution along the whole flux tube in the presence of the special $\vec{E}_{\parallel}$ fields. On the other hand, the observed lack of initial westward motion during the first 30 seconds might also be explained as due to the relatively high electron density at these initial times, thus reducing the westward $-c\vec{J}_{\perp}/eN$ component of $\vec{V}_{\perp f}$ in Equation 12. At subsequent times, beta-deposition decreases and so N also decreases, while $\vec{J}_{\perp}$ remains large at 85 km altitude, thus allowing the beta-tube foot-points to drift westward. From this point of view, special $\vec{E}_{\parallel}$ fields would not be required. A very detailed 3-D computation of the Kingfish and Checkmate plasma evolution during the first five minutes after the bursts seems necessary to resolve whether or not special $\vec{E}_{\parallel}$ fields are required to explain the nuclear burst observations.

If the above special $\vec{E}_{\parallel}$ fields cannot develop in nuclear burst striations, then it seems likely that long striations will gradually shear across adjacent flux tubes in those regions of the striation where $\vec{J}_{\perp}$ is non-zero, with a transverse-to-B shearing velocity equal to $c\vec{J}_{\perp}/eN$. The effect on the striated nuclear burst plasma would be to decrease the mean electron density $\overline{N}$ and rms electron density fluctuations σ_N at very high altitudes, to increase the $\overline{N}$ and σ_N at ionospheric altitudes, and to accelerate the overall plasma decay due to the more rapid molecular chemistry at ionospheric heights.

REFERENCES

1. W. A. Newcomb, "Motion of Magnetic Lines of Force", Annals of Physics, 3, 347-385 (1958), Academic Press.

2. C. L. Longmire, "Elementary Plasma Physics", pp. 34-40, Interscience Publishers/John Wiley, New York, 1963

3. C. L. Longmire and R. W. Kilb, pp. 617-621 of "Plasma Physics", Chapter 12 in "Physics of High-Altitude Nuclear Burst Effects", DNA4501F, Mission Research Corporation, December 1977.

4. T. J. Hallinan, pp. 42-49, in "Physics of Auroral Arc Formation", edited by S. I. Akasofu and J. R. Kan, American Geophysical Union, Washingon D.C. 1981.

5. R. W. Kilb, "Kinked Magnetic Fields, $E_{\parallel}$ -fields, and Westward Displacement of Beta-Tubes", in Volume II of DNA Proceedings of 1982 La Jolla Meeting.

6. M. Scholer, "On the Motion of Artificial Ion Clouds in the Magnetosphere", in Planetary and Space Science, 18, pp. 977-1004 (1970), Pergamon Press.

7. J. L. Sperling, "Ion Pedersen Drift and Parallel Electric Field Effects On Plasma Jetting", DNAxxxxx, JAYCOR, October 1982. Also to be published in J. of Geophys. Research (1983).

APPENDIX

MOST SIMPLE VERSION OF IONOSPHERIC PLASMA EQUATIONS

Several coworkers have suggested to me that it would be more obvious and convincing that $\vec{V}_{i\perp}\cdot\vec{J}_\perp$ is negligible compared to $\vec{V}_{e\perp}\cdot\vec{J}_\perp$ (i.e., that the electrons primarily carry the current transverse-to-B relative to the neutrals) if this were proved using the standard $\vec{E}_\perp$ and $\vec{E}_\perp\times\vec{b}$ basis vectors for $\vec{V}_{i\perp}$, $\vec{V}_{e\perp}$ and $\vec{J}_\perp$. Let us therefore use a local reference frame moving with the neutral fluid so $\vec{V}_0=0$. We also neglect electron collisions ($\eta_{eo}=0$ and $\eta_{ei}=0$), ion inertia, $\nabla(P_i+P_e)$, $\vec{g}$, etc. Keeping only ion-neutral collisions (η_{io}), Equations 12-133, 12-134, and 12-135 yield the standard formulas for this most simple ionospheric plasma motion:

$$\vec{V}_{i\perp} \approx \frac{1}{1+\eta_{io}^2}\cdot\frac{c}{B}\vec{E}_\perp\times\vec{b} + \frac{\eta_{io}}{1+\eta_{io}^2}\cdot\frac{c}{B}\vec{E}_\perp \qquad (I.1)$$

$$\vec{V}_{e\perp} \approx \frac{c}{B}\vec{E}_\perp\times\vec{b} \qquad (I.2)$$

$$\vec{J}_\perp \approx \frac{\eta_{io}}{1+\eta_{io}^2}\cdot\frac{eN}{B}\vec{E}_\perp - \frac{\eta_{io}^2}{1+\eta_{io}^2}\cdot\frac{eN}{B}\vec{E}_\perp\times\vec{b} \qquad (I.3)$$

Taking the dot product of $\vec{J}_\perp$ with $\vec{V}_{i\perp}$ and $\vec{V}_{e\perp}$, we then find:

$$\vec{J}_\perp\cdot\vec{V}_{i\perp} = \frac{\eta_{io}^2}{(1+\eta_{io}^2)^2}\cdot\frac{ceN}{B^2}E_\perp^2 - \frac{\eta_{io}^2}{(1+\eta_{io}^2)^2}\cdot\frac{ceN}{B^2}E_\perp^2 = 0 \qquad (I.4)$$

$$\vec{J}_\perp\cdot\vec{V}_{e\perp} = -\frac{\eta_{io}^2}{1+\eta_{io}^2}\cdot\frac{ceN}{B^2}E_\perp^2 = -\frac{\eta_{io}^2}{1+\eta_{io}^2}\cdot\frac{eN}{c}V_{e\perp}^2 = -\frac{c}{eN}J_\perp^2 \qquad (I.5)$$

Therefore only the electrons move in direction of $\vec{J}_\perp$ relative to the neutrals. The ions do not move in direction of $\vec{J}_\perp$, but do move in direction of $\vec{J}_\perp \times \vec{b}$ relative to the neutrals. This is consistent with Equations 10 and 11 of Section 2; those equations are more general in that they also include the effect of electron collisions, but since $n_{io} \approx 1000 n_{eo}$, it is clear that the electrons are the primary current carrier transverse-to-B as well as parallel-to-B.

Figure I-1 shows a pictorial version of Equations I-1, I-2, and I-3 suggested to the author by C. Longmire. We have drawn the vector diagrams for various n_{io} values (i.e., for various ionospheric altitudes) and adjusted the $\vec{E}_\perp$ magnitude and direction so that $\vec{V}_{i\perp}$ is the same at all altitudes (i.e., for all n_{io} values). Note that the $\vec{J}_\perp$ vector is always perpendicular to $\vec{V}_{i\perp}$ and points in the same direction at all altitudes in this simple example wherein $\vec{V}_0 = 0$. Thus in this simple case the ion column moves as a unit transverse-to-B, but the electric field cannot be taken as an equipotential because $\vec{E}_\perp$ rotates and changes its magnitude at the various altitudes (i.e., various n_{io} values).

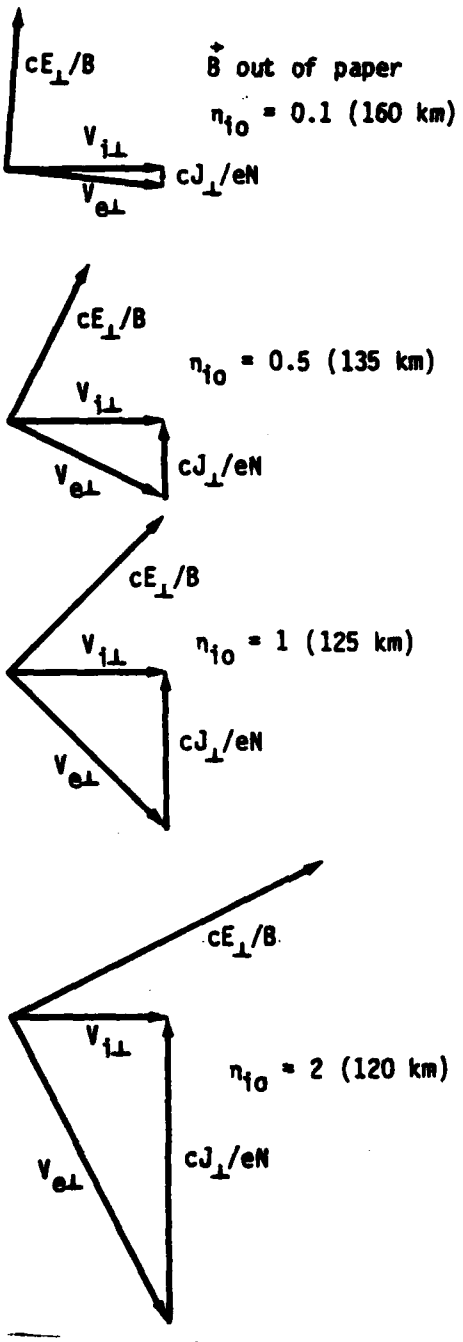

Figure I-1. Relationship between $\vec{V}_{i\perp}$, $\vec{V}_{e\perp}$, $c\vec{E}_\perp/B$, and $c\vec{J}_\perp/eN$ at various altitudes. $\vec{V}_{i\perp}$ has been chosen to have the same direction and magnitude at all altitudes; this then requires that $\vec{E}_\perp$ rotates clockwise and increases in magnitude (as $\sqrt{1+n_{io}^2}$) as one descends in altitude. Note that $\vec{J}_\perp$ is always perpendicular to $\vec{V}_{i\perp}$. Here it has been assumed that $\vec{V}_\theta=0$ at all altitudes.

ADDENDUM: Pages 617-621 from DNA4501F

12.4.4 LOW-β PLASMAS ABOVE 100 KM ALTITUDE

In the normal ionospheric E and F-layers the ion-electron pressure P is much less than the magnetic pressure $B^2/8\pi$. The ratio $8\pi P/B^2$ is often referred to as the plasma-β. Such low-β plasmas also occur after a few minutes subsequent to high altitude nuclear bursts and for barium cloud releases in the ionosphere. Under these conditions it is not possible energetically to cause substantial distortions of the magnetic field. Thus $\partial\vec{B}/\partial t$ is very small, and as a consequence of Maxwell's Equation (12-2), the electric field must be primarily electrostatic. Experience with numerical computations shows that it is very difficult to accurately solve the magnetohydrodynamic Equations (12-100) through (12-107) when the plasma-β is small. One must recast these equations to obtain a more viable procedure for finding a solution (Ref. 12-4).

A key point is that currents will be induced in the high altitude plasma as it moves about in response to the applied forces such as gravity, neutral winds, pressure gradients, etc. The effect of these currents is to average the applied forces along each field line via $\vec{J}\times\vec{B}$ forces such that essentially all of the electrons in a given magnetic flux tube will $\vec{E}\times\vec{B}$ drift together to another field-aligned flux tube. Because only a negligibly small space-charge is needed to set up the spatially varying electrostatic field $\vec{E}$ that causes the $\vec{E}\times\vec{B}$ drift of the plasma, it is crucial that the current density $\vec{J}$ be essentially divergence-free, i.e., that:

$$\nabla\cdot\vec{J} = 0 \qquad (12\text{-}123)$$

To employ this equation we must express $\vec{J}$ in terms of the electric field and the forces acting on the plasma. For the conditions discussed in this subsection, the ion-electron plasma is collisional because the plasma evolves on a time scale of minutes and the expected plasma temperature-density parameters are in the range of less than 0.1 eV at $10^4 cm^{-3}$ to

less than 2 eV at $10^9 cm^{-3}$. On the other hand, above 100 km altitude, collisions with neutrals are insufficient to provide tight coupling with the neutral fluid. Thus we must employ a multi-fluid description, with the neutrals, the ions, and the electrons obeying the following momentum conservation equations:

$$\frac{\partial \rho_o \vec{V}_o}{\partial t} + \nabla \cdot (\rho_o \vec{V}_o \vec{V}_o) = - \nabla P_o + \rho_o \vec{g} - \nu_{io} \rho_i (\vec{V}_o - \vec{V}_i) - \nu_{eo} \rho_e (\vec{V}_o - \vec{V}_e) \qquad (12\text{-}124)$$

$$\frac{\partial (\rho_i \vec{V}_i)}{\partial t} + \nabla \cdot (\rho_i \vec{V}_i \vec{V}_i) = - \nabla P_i + \rho_i \vec{g} + eN_i (\vec{E} + \vec{V}_i \times \vec{B}/c)$$

$$+ \nu_{io} \rho_i (\vec{V}_o - \vec{V}_i) - \nu_{ei} \rho_e (\vec{V}_i - \vec{V}_e) \qquad (12\text{-}125)$$

$$\frac{\partial (\rho_e \vec{V}_e)}{\partial t} + \nabla \cdot (\rho_e \vec{V}_e \vec{V}_e) = - \nabla P_e + \rho_e \vec{g} - eN_e (\vec{E} + \vec{V}_e \times \vec{B}/c)$$

$$+ \nu_{eo} \rho_e (\vec{V}_o - \vec{V}_e) + \nu_{ei} \rho_e (\vec{V}_i - \vec{V}_e) \qquad (12\text{-}126)$$

The subscripts o, i, and e respectively indicate neutral, ion, and electron fluid parameters. The ion-neutral, electron-neutral, and electron-ion collision frequencies are denoted by ν_{io}, ν_{eo}, and ν_{ei}. Detailed calculations of these collision frequencies for nuclear burst conditions are given in Ref. 12-5; approximate values are indicated in the glossary of Chapter 13 of this compendium.

The terms involving ν_{io}, ν_{eo}, and ν_{ei} in the three above equations account for momentum transfer between the three fluids via collisions. In Equation (12-124), the last term is negligible compared to the others. The usual magnetohydrodynamic equation is obtained by adding Equations (12-125) and (12-126). Neglecting some small terms, this yields:

$$\frac{\partial(\rho_i \vec{V}_i)}{\partial t} + \nabla\cdot(\rho_i \vec{V}_i \vec{V}_i) = -\nabla(P_i+P_e) + \rho_i \vec{g} + \vec{J}\times\vec{B} + \nu_{io}\rho_i(\vec{V}_o-\vec{V}_i) \qquad (12\text{-}127)$$

Equations (12-124) and (12-127), together with (12-106) and (12-107), are referred to as the two-fluid MHD equations.

Returning now to the problem of obtaining a suitable expression for $\vec{J}$, we will solve Equations (12-125) and (12-126) for $\vec{V}_i$ and $\vec{V}_e$ and then find $\vec{J}$ from

$$\vec{J} = \frac{eN}{c}(\vec{V}_i-\vec{V}_e) \qquad (12\text{-}128)$$

To solve those two equations for the transverse-to-$\vec{B}$ velocity components $\vec{V}_{i\perp}$ and $\vec{V}_{e\perp}$ we introduce the auxiliary notation:

$$\vec{A}_i \equiv \nabla P_i - \rho_i \vec{g} + \frac{\partial(\rho_i \vec{V}_i)}{\partial t} + \nabla\cdot(\rho_i \vec{V}_i \vec{V}_i) \qquad (12\text{-}129)$$

$$\vec{A}_e \equiv \nabla P_e - \rho_e \vec{g} + \frac{\partial(\rho_e \vec{V}_e)}{\partial t} + \nabla\cdot(\rho_e \vec{V}_e \vec{V}_e) \qquad (12\text{-}130)$$

$$\eta_{io} \equiv \nu_{io}/\Omega_i; \qquad \eta_{eo} = \nu_{eo}/\Omega_e; \qquad \eta_{ei} = \nu_{ei}/\Omega_e \qquad (12\text{-}131)$$

$$d \equiv (1+\eta_{io}^2)(1+\eta_{eo}^2) + \eta_{ei}(\eta_{io}+\eta_{eo})\,[2+2\eta_{io}\eta_{eo}+\eta_{ei}(\eta_{io}+\eta_{eo})] \qquad (12\text{-}132)$$

where the η's are the ratios of the collision frequencies to the appropriate gyro-frequency. These η's are all positive numbers. For nuclear burst conditions, η_{eo} and η_{io} are less than unity above about 70 km and 130 km altitude respectively, and they are nearly proportional to the neutral fluid density. At any particular point the ratio η_{eo}/η_{io} is small and about equal to 1/1000. The η_{ei} is proportional to N_e and

outside fireballs the η_{ei} is generally smaller than η_{eo} at altitudes below 200 km. Above 300 km altitude, or inside fireballs, η_{ei} is usually larger than η_{eo} and may also be larger than η_{io}. At altitudes above about 150 km d is approximately unity because η_{io}, η_{eo}, and η_{ei} are generally small at high altitudes.

The exact solutions for $\vec{V}_{i\perp}$ and $\vec{V}_{e\perp}$ are obtained by inverting a 4×4 matrix, with the result that

$$\begin{aligned}
\vec{V}_{i\perp}d = {} & \left[1+\eta_{eo}^2+\eta_{ei}(\eta_{io}+\eta_{eo})\right] \frac{c}{B} \left(\vec{E}_\perp + \frac{1}{eN}\vec{A}_{e\perp}\right)\times\vec{b} \\
& + \left[\eta_{io}(1+\eta_{eo}^2) + \eta_{ei}\eta_{eo}(\eta_{io}+\eta_{eo})\right]\left[\frac{c}{B}\left(\vec{E}_\perp + \frac{1}{eN}\vec{A}_{e\perp}\right) + \vec{V}_o\times\vec{b}\right] \\
& + \left[\eta_{io}^2(1+\eta_{eo}^2) + \eta_{ei}(\eta_{io}+\eta_{eo})\left[1+2\eta_{io}\eta_{eo}+\eta_{ei}(\eta_{io}+\eta_{eo})\right]\right]\vec{V}_{o\perp} \\
& - \left[\eta_{io}(1+\eta_{eo}^2) + \eta_{ei}\left[1+\eta_{eo}^2+2\eta_{io}\eta_{eo}+\eta_{ei}(\eta_{io}+\eta_{eo})\right]\right] \frac{c}{eNB}\left(\vec{A}_i+\vec{A}_e\right)_\perp \\
& + \left[1+\eta_{eo}^2+2\eta_{eo}\eta_{ei}\right] \frac{c}{eNB}\vec{b}\times(\vec{A}_i+\vec{A}_e)
\end{aligned} \tag{12-133}$$

$$\begin{aligned}
\vec{V}_{e\perp}d = {} & \left[1+\eta_{io}^2+\eta_{ei}(\eta_{io}+\eta_{eo})\right] \frac{c}{B} \left(\vec{E}_\perp + \frac{1}{eN}\vec{A}_{e\perp}\right)\times\vec{b} \\
& - \left[\eta_{eo}(1+\eta_{io}^2) + \eta_{ei}\eta_{io}(\eta_{io}+\eta_{eo})\right]\left[\frac{c}{B}\left(\vec{E}_\perp + \frac{1}{eN}\vec{A}_{e\perp}\right) + \vec{V}_o\times\vec{b}\right] \\
& + \left[\eta_{eo}^2(1+\eta_{io}^2) + \eta_{ei}(\eta_{io}+\eta_{eo})\left[1+2\eta_{io}\eta_{eo}+\eta_{ei}(\eta_{io}+\eta_{eo})\right]\right]\vec{V}_{o\perp} \\
& - \eta_{ei}\left[1+\eta_{io}\eta_{eo}+\eta_{ei}(\eta_{io}+\eta_{eo})\right] \frac{c}{eNB}\left(\vec{A}_i+\vec{A}_e\right)_\perp \\
& - \eta_{ei}(\eta_{io}-\eta_{eo}) \frac{c}{eNB}\vec{b}\times(\vec{A}_i+\vec{A}_e)
\end{aligned} \tag{12-134}$$

Using these expressions for $\vec{V}_{i\perp}$ and $\vec{V}_{e\perp}$ in Equation (12-128), we obtain:

$$\frac{c\vec{J}_{\perp d}}{eN} = -(\eta_{io}^2-\eta_{eo}^2)\left[\frac{c}{B}(\vec{E}_\perp + \frac{1}{eN}\vec{A}_{e\perp})\times\vec{b} - \vec{V}_{o\perp}\right]$$

$$+ (\eta_{io}+\eta_{eo})\left[1+\eta_{io}\eta_{eo}+\eta_{ei}(\eta_{io}+\eta_{eo})\right]\left[\frac{c}{B}(\vec{E}_\perp + \frac{1}{eN}\vec{A}_{e\perp}) + \vec{V}_o\times\vec{b}\right]$$

$$-\left[\eta_{io}(1+\eta_{eo}^2) + \eta_{ei}\eta_{eo}(\eta_{io}+\eta_{eo})\right]\frac{c}{eNB}(\vec{A}_i+\vec{A}_e)_\perp$$

$$+\left[1+\eta_{eo}^2+\eta_{ei}(\eta_{io}+\eta_{eo})\right]\frac{c}{eNB}\vec{b}\times(\vec{A}_i+\vec{A}_e) \qquad (12\text{-}135)$$

Equations (12-125) and (12-126) may also be solved for the parallel-to-$\vec{B}$ current density $\vec{J}_\parallel$:

$$\frac{c}{eN}\left[\eta_{eo} + \eta_{ei}\left(1+\frac{\eta_{eo}}{\eta_{io}}\right)\right]\vec{J}_\parallel = \left(1+\frac{\eta_{eo}}{\eta_{io}}\right)\frac{c}{B}\left(\vec{E}_\parallel + \frac{1}{eN}\vec{A}_{e\parallel}\right) - \frac{\eta_{eo}}{\eta_{io}}\frac{c}{eNB}\left(\vec{A}_i+\vec{A}_e\right)_\parallel$$

(12-136)

No approximations have been made in deriving Equations (12-133)-(12-136) from the MHD Equations (12-125) and (12-126) except the negligible one that $N_i=N_e=N$. In particular, the $\vec{E}$ fields appearing in these equations could be inductive as well as electrostatic.

DISTRIBUTION LIST

DEPARTMENT OF DEFENSE

Defense Nuclear Agency
ATTN: NATO
ATTN: RAEE
ATTN: STNA
ATTN: RAAE, P. Lunn
ATTN: NAFD
3 cy ATTN: RAAE
4 cy ATTN: TITL

Defense Tech Info Ctr
12 cy ATTN: DD

DEPARTMENT OF THE NAVY

Naval Research Lab
ATTN: Code 4780, S. Ossakow
ATTN: Code 4108, E. Szuszewicz
ATTN: Code 4720, J. Davis
ATTN: Code 6700
ATTN: Code 7950, J. Goodman
ATTN: Code 4780
ATTN: Code 7500, B. Wald
ATTN: Code 4187
ATTN: Code 4700

DEPARTMENT OF THE AIR FORCE

Air Force Geophysics Lab
ATTN: LYD, K. Champion
ATTN: OPR-1
ATTN: R. Babcock
ATTN: CA, A. Stair
ATTN: OPR, H. Gardiner
ATTN: PHY, J. Buchau
ATTN: R. O'Neil

Air Force Weapons Lab
ATTN: SUL
ATTN: NTN

DEPARTMENT OF ENERGY CONTRACTORS

Los Alamos National Lab
ATTN: MS 670, J. Hopkins
ATTN: P. Keaton
ATTN: D. Simons
ATTN: MS 664, J. Zinn
ATTN: T. Kunkle, ESS-5
ATTN: J. Wolcott
ATTN: R. Jeffries

DEPARTMENT OF DEFENSE CONTRACTORS

Berkeley Rsch Associates, Inc
ATTN: J. Workman
ATTN: C. Prettie
ATTN: S. Brecht

JAYCOR
ATTN: J. Sperling

Kaman Sciences Corp
ATTN: E. Conrad

DEPARTMENT OF DEFENSE CONTRACTORS (Continued)

Kaman Tempo
ATTN: DASIAC

Kaman Tempo
ATTN: DASIAC

Mission Research Corp
ATTN: G. McCartor
ATTN: D. Knepp
ATTN: R. Bogusch
ATTN: F. Guigliano
ATTN: F. Fajen
ATTN: Tech Library
ATTN: R. Bigoni
ATTN: R. Dana
ATTN: S. Gutsche
ATTN: R. Hendrick
4 cy ATTN: C. Lauer
4 cy ATTN: R. Kilb
5 cy ATTN: Doc Con

Pacific-Sierra Rsch Corp
ATTN: H. Brode, Chairman SAGE

Physical Dynamics, Inc
ATTN: J. Secan
ATTN: E. Fremouw

Physical Research, Inc
ATTN: T. Stevens
ATTN: R. Deliberis
ATTN: J. Devore
ATTN: K. Schwartz

R&D Associates
ATTN: G. Stoyr
ATTN: M. Gantsweg
ATTN: W. Karzas
ATTN: C. Greifinger
ATTN: F. Gilmore
ATTN: W. Wright
ATTN: R. Turco
ATTN: H. Ory
ATTN: P. Haas

R&D Associates
ATTN: B. Yoon

SRI International
ATTN: A. Burns
ATTN: G. Price
ATTN: R. Tsunoda
ATTN: J. Vickrey
ATTN: V. Gonzales
ATTN: J. Petrickes
ATTN: M. Baron
ATTN: R. Livingston
ATTN: D. Neilson
ATTN: D. McDaniels
ATTN: W. Chesnut
ATTN: G. Smith
ATTN: W. Jaye
ATTN: R. Leadabrand
ATTN: C. Rino

DEPARTMENT OF DEFENSE CONTRACTORS (Continued)

Visidyne, Inc
ATTN: W. Reidy
ATTN: J. Carpenter
ATTN: O. Shepard
ATTN: C. Humphrey

DEPARTMENT OF DEFENSE CONTRACTORS (Continued)

Toyon Research Corp
ATTN: J. Ise
ATTN: J. Garbarino